

# Description of Unsteady Flows in the Cuboid Container

K. Horáková, K. Fraňa, V. Honzejk

## II. LORENTZ FORCES IN THE CONTAINER

### A. Problem Formulation

Input data for descriptions of this unsteady flow in the cuboid container were obtained from the in-house code (called NS-FEM3D) which uses DDES method of computing. The Delayed Detached Eddy Simulation model has been applied as a turbulent approach. This approach was implemented for higher Taylor number. Without any turbulent approach study of unsteady flows driven by magnetic field was limited only for lower Taylor number. This code is based on the finite-element method with a pressure stabilized Petrov-Galerkin and streamline upwind Petrov-Galerkin approach. Complete summary of applied mathematical model and validations see in [8], [9].

Input data from the code contain – coordinates of grid node points, values of Lorentz forces component (or more precisely form of accelerations) in the Cartesian coordinate system and this database was processed in software MathCad (version 15).

The grid of container was unstructured. Whole grid has over 2 200 000 elements. Because of unstructured grid weighting function was chosen. Lorentz force values in current planes were determined by weighting function of four real grid points (the nearest point has the biggest weight, the most distant grid point has the lowest weight). For more details about this weighting function see in author's earlier works [10], [11].

The current container is considered with electrically isolated walls, the melt inside the container is electrically conductive with density  $\rho$ , kinematic viscosity  $\nu$  and electric conductivity  $\sigma$ . Flow of the melt is driven by rotating magnetic field with magnetic induction  $B$ . Magnetic induction has only components  $B_x$  a  $B_y$ , it is assumed that vertical size of bipolar inductor is bigger than the height of the melt in the container.

The sketch of the flow problem is illustrated in Fig. 1. The principle of electromagnetic stirring is the same as the principle of an induction motor. The base of function is creation of rotating magnetic field (RMF). This field is generated by passing of alternating current to stator winding (inductor). Magnetic field induces tension in the rotor (melt) and caused electric current elicits forces. These forces (Lorentz forces) cause rotation of rotor (melt). Varying magnetic field around the coil is generated in the circuit of alternating current. This magnetic field induces open circuit voltage in the coil.

**Abstract**—This part of study deals with description of unsteady isothermal melt flow in the container with cuboid shape. This melt flow is driven by rotating magnetic field. Input data (instantaneous velocities, grid coordinates and Lorentz forces) were obtained from in-house CFD code (called NS-FEM3D) which uses DDES method of computing. Description of the flow was performed by contours of Lorentz forces and caused velocity field. Taylor magnetic numbers of the flow were used  $1.10^6$ ,  $5.10^6$  and  $1.10^7$ , flow was in 3D turbulent flow regime.

**Keywords**—In-house computing code, Lorentz forces, magnetohydrodynamics, rotating magnetic field.

## I. INTRODUCTION

**M**AGNETOHYDRODYNAMICS (MHD for short) is a theory of interaction between magnetic field and moving, conducting fluids [1].

Using of the rotating magnetic field (RMF) is mostly surveyed in recent years. In a few papers were compared static and rotating magnetic fields [2]. The rotating magnetic field was turned out like better usable. In next papers the flow stability and formation instabilities were monitored [3]. In the work of Dold a Benze [2] the experimental reduction of the temperature fluctuations in the case of crystal growth was described. RMF is testing for using gallium and for different metallographic technics (Float Zone, Czochralski, Bringman nebo Travelling Heater Method) [4, etc]. Production of semiconductors is another possibility of using magnetic field [5], [6]. Magnetic field is exploited also in magnetic damping, levitation melting etc. [7], [1].

The subject of this work is a description of the melt flow inside of the container. The melt is electrically conductive and the container has cuboid shape. The flow of the melt is driven by rotating magnetic field. In Navier-Stokes equations for flow calculations there occurred the external forces. In the flow of melt driven by a rotating magnetic field these forces are the Lorentz forces. Theme of this article is description of Lorentz forces contours for different Taylor numbers in whole cuboid container. Caused time-averaged velocity field is displayed and described as well.

K. Horáková is with The Faculty of Mechanical Engineering of Technical University of Liberec, Department of Power Engineering Equipment, Liberec, Czech Republic (phone: 00420 48 535 3434; e-mail: katerina\_horakova@centrum.cz).

K. Fraňa is with The Faculty of Mechanical Engineering of Technical University of Liberec, Department of Power Engineering Equipment, Liberec, Czech Republic (phone: 00420 48 535 3436; e-mail: karel.frana@seznam.cz).

V. Honzejk is with The Faculty of Mechanical Engineering of Technical University of Liberec, Department of Power Engineering Equipment, Liberec, Czech Republic.

This work was financial supported from the particular research student grant SGS 28000 at the TU of Liberec.

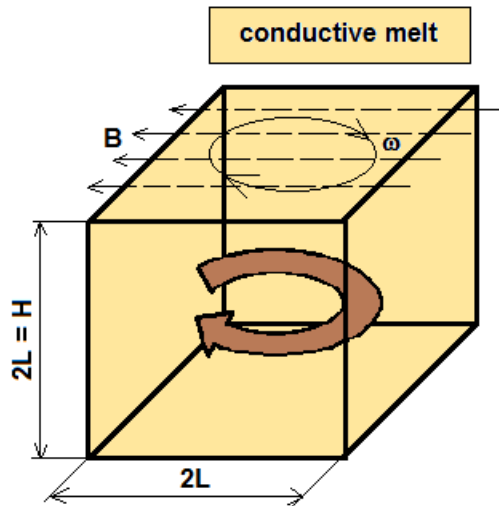


Fig. 1 The sketch of the flow problem

Lorentz forces have generally sum of time-dependent and the mean part. However frequency of rotating magnetic field is large enough so that oscillative part of Lorentz forces could be neglected with regard to mean part [12]. Oscillative part of Lorentz forces rotate with double frequency. The melt could not achieve that large difference of Lorentz force part because of her large inertia [3]. To prescribe forces the low-frequency and the low-induction condition are assumed.

Contours of Lorentz forces in different plane are displayed in Figs. 2–4. Taylor magnetic number of this flow is  $Ta = 1.10^6$ . Only Lorentz forces in azimuthal direction was monitored. This part of Lorentz forces (azimuthal) is dominant. Lorentz forces were divided by maximum value of the Lorentz forces (in whole container) before displaying, so that contours of Lorentz forces are non-dimensional – normalized. The range of Lorentz forces values is from zero to one. Maxima of Lorentz forces are displayed by red color, minima by violet color.

#### B. Contours of Lorentz Forces in Central Plane

Forces in central plane (it goes through vertical axis and it is perpendicular to lateral side of cuboid container) are displayed in Fig. 2. In horizontal axis non-dimensional edge of the container  $x'(-)$  is used. That means edge  $L(m)$  was divided by half of container height  $L(m)$ . Because of symmetry only half of the container section is displayed (in central and cross plane). In vertical axis non-dimensional height of the container  $z'(-)$  is used. It means height  $z(m)$  was divided half of container height  $L(m)$ . Axis of symmetry is situated on the left of Fig. 2.

With increasing distance from vertical axis values of Lorentz forces are larger (in half of the container height). It is apparently caused by larger mass so that momentum is larger. Maxima of Lorentz forces are occurred on the outer walls in the half of container height. On the contrary minima of magnetic forces are in the axis of container (small distance

from vertical axis so that smaller momentum) and on upper and lower base (based on boundary conditions).

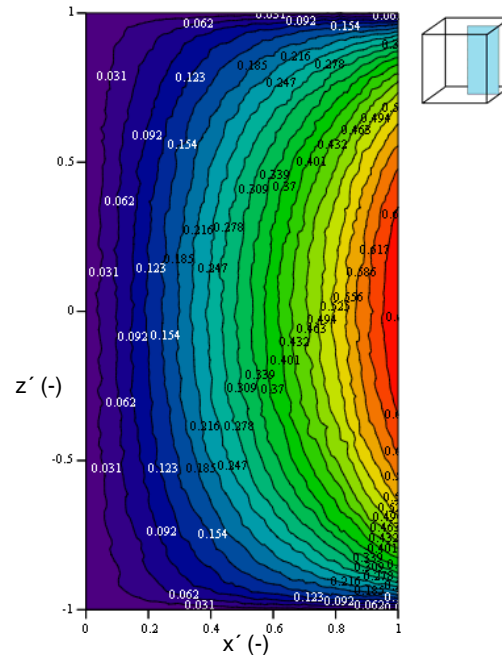


Fig. 2 Contours of time – averaged Lorentz forces in azimuthal direction in central plane

#### C. Contours of Lorentz Forces in Cross Plane

Lorentz forces in cross plane are displayed in Fig. 3. In horizontal axis of Fig. 3 non-dimensional edge of the container  $xy'(-)$  is used. That means cross edge  $xy(m)$  (that is  $L(m)/\sin(45^\circ)$ ) was divided by half of container height  $L(m)$ . Vertical axis is the same as in Fig. 2. Maxima of Lorentz forces were obtained near corners of the container (or more precisely near container vertical edges). It is apparently caused by larger mass so that momentum is larger.

#### D. Contours of Lorentz Forces in Horizontal Plane

Lorentz forces in horizontal plane are displayed in Fig. 4. In horizontal axis non-dimensional edge of the container  $x'(-)$  is used. In vertical axis non-dimensional edge of the container  $y'(-)$  is used. That means edge  $L(m)$  was divided by half of container height  $L(m)$ . With increasing distance from vertical axis values of Lorentz forces are larger. Twenty one contours are displayed.

### III. VELOCITY FIELD IN THE CONTAINER

Lorentz forces cause melt moving dominantly in azimuthal direction. Contours of velocities correspond with contours of Lorentz forces.

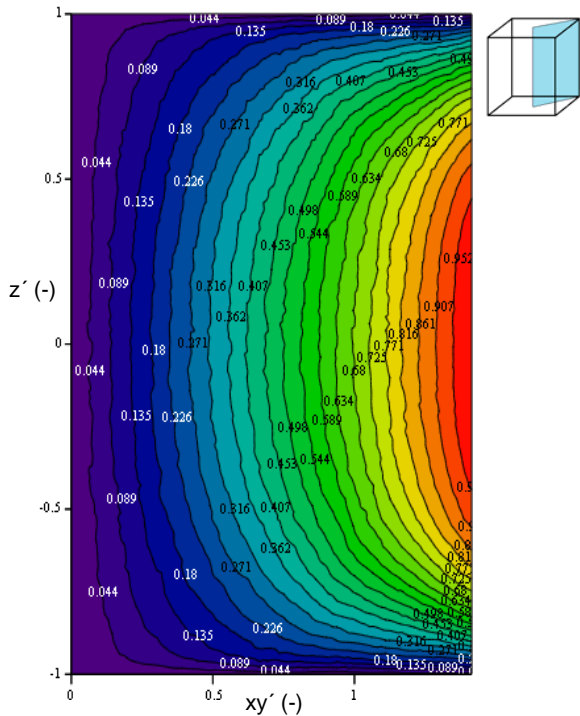


Fig. 3 Contours of time – averaged Lorentz forces in azimuthal direction in cross plane

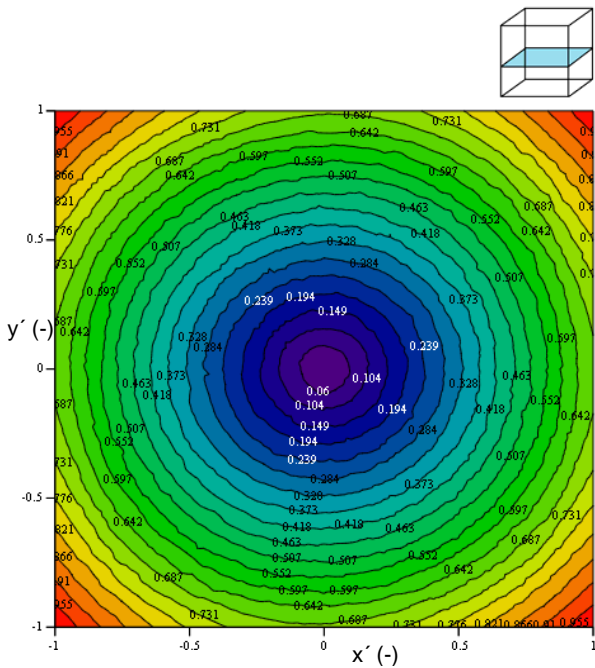


Fig. 4 Contours of time – averaged Lorentz forces in azimuthal direction in horizontal plane

Contours of time – averaged velocities are displayed in Figs. 5-7. Input data for data processing were obtained from home-made computing code NS-FEM3D [8], [9]. Values

of velocities for displaying were determined by weighting function of four real grid points as well (the nearest point has the biggest weight; the most distant grid point has the lowest weight). Data processing and displaying were performed in MathCad (version 15) as well as Lorentz forces.

A. Velocities in Central Plane

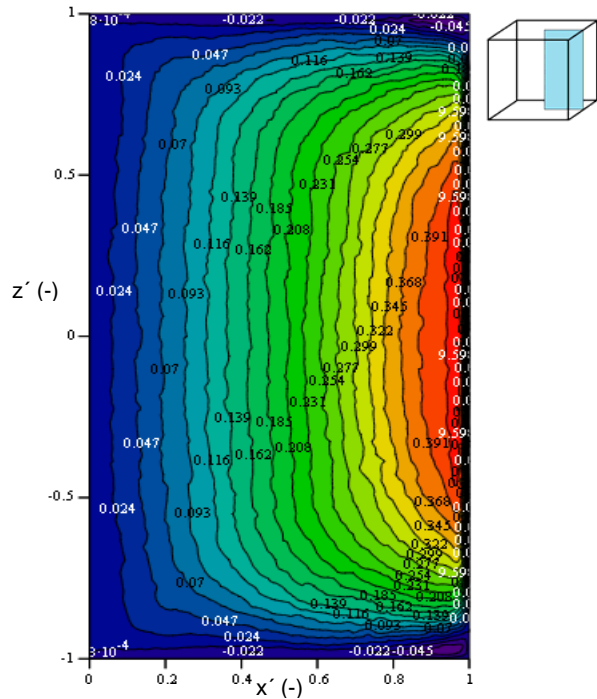


Fig. 5 Contours of time – averaged azimuthal velocities in central plane for  $Ta = 1.10^6$

Fig. 5 shows contours of time – averaged azimuthal velocities in central plane of cuboid container. Velocities in azimuthal direction are dominant. In horizontal axis and vertical axis non-dimensional cuboid edge size  $x'(-)$  and  $z'(-)$  are used as well as on Lorentz forces. Because of symmetry only half of the container section is displayed. Axis of symmetry is situated on the left of Fig. 5. Shapes of contours correspond with contours of Lorentz forces displayed in the same plane. Velocity field is caused by these Lorentz forces. Taylor number of this flow is  $Ta = 10^6$ . Maximum velocity is occurred on the outer walls in the half of container height. On the contrary minimum velocity is occurred in the axis of container and on upper and lower base (based on boundary conditions). Because of container shape (cuboid container) velocity in vertical axis is not zero. Moving melt (dominantly in azimuthal direction) accelerates and decelerates (from smaller to bigger distance from vertical axis in horizontal plane) and relatively significant turbulent structures are appeared. Near lower and upper bases melt is affected by edges and friction.

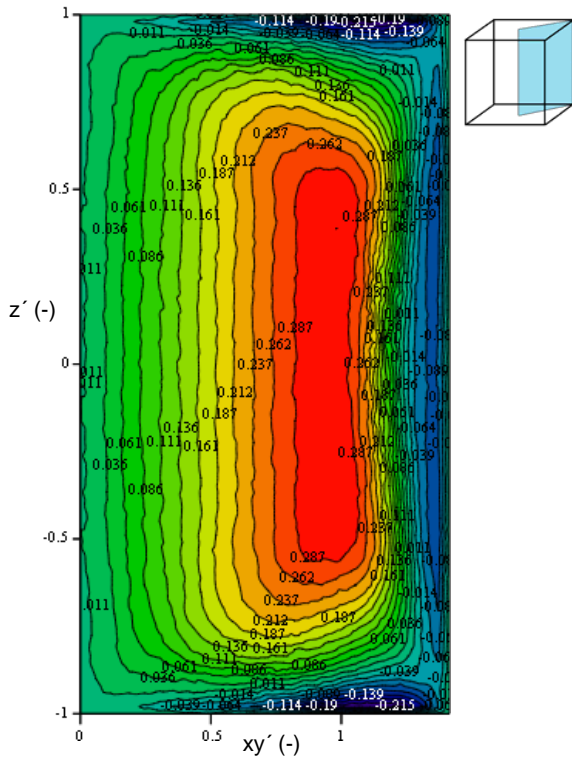


Fig. 6 Contours of time – averaged azimuthal velocities in cross plane for  $Ta = 1.10^6$

Contours of time – averaged azimuthal velocities in cross plane are displayed in Fig. 6. In horizontal axis non-dimensional edge of the container  $xy'(-)$  is used as well as on Lorentz forces. Vertical axis is non-dimensional as well.

Maximum velocity is occurred approximately near radius of hypothetical in-cylinder (near non-dimensional value of 1 in horizontal axis). But value of this maximum is smaller than maximum velocity in central plane. The melt is accelerated in narrower cross-section (smaller distance from vertical axis in horizontal plane) and decelerated in wider cross-section (bigger distance from vertical axis in horizontal plane). Whole velocity field is slightly drafted to container edges. Near upper and lower bases and vertical container walls slight reversing of the flow was appeared and small eddies were formed.

Effect of container shape is most obvious in Fig. 7. Contours of time – averaged azimuthal velocities in horizontal plane are displayed (in half of the container height).

Velocity field is not fully symmetrical. The melt is accelerated near vertical container wall and decelerated near container edges. Whole velocity field is slightly drafted to container edges. Minimum velocity is occurred near vertical axis and container edges.

Small corner eddies near vertical container edges should be detected after displaying velocity field with absolute value of velocity. This corresponds to published results in author's earlier works, where was described dependence power spectrum of kinetic energy on wave number for lines near

corners, see [13]. These small corner eddies have much lower energy than mean flow and these eddies are absorbed by him.

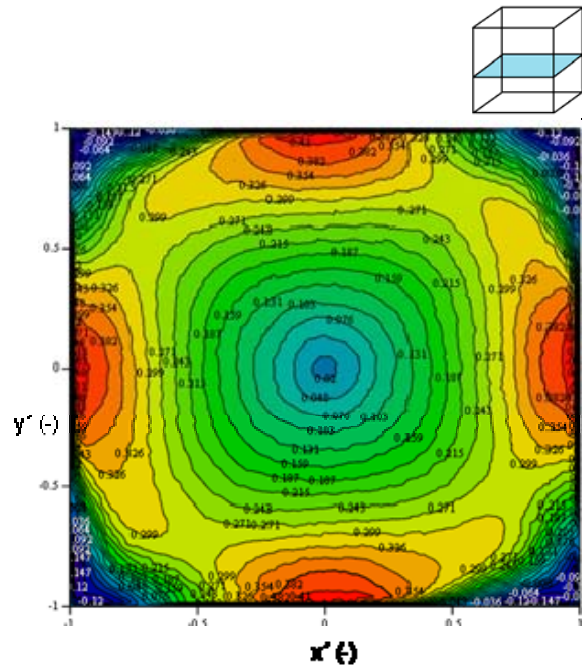


Fig. 7 Contours of time – averaged azimuthal velocities in horizontal plane for  $Ta = 1.10^6$

#### IV. DIFFERENT TAYLOR NUMBER

##### A. Lorentz Forces for Different Taylor Number

Taylor magnetic number is defined as:

$$Ta = \frac{\sigma \cdot \varpi \cdot B_0^2 \cdot L^4}{2 \cdot \rho \cdot \nu^2} \quad (1)$$

where  $B_0$  is amplitude of magnetic induction,  $\varpi$  is angular velocity of magnetic field,  $L$  is the half of container edge,  $\rho$  is melt density,  $\nu$  is kinematic viscosity and  $\sigma$  is electric conductivity of melt.

Contours of Lorentz forces for higher Taylor number are very similar, only values of Lorentz forces are much larger. Dependence of time-averaged Lorentz forces (in azimuthal direction) on non-dimensional height of the container is displayed in Fig. 8. In horizontal axis non-dimensional  $x'(-)$  is used. The dependence for line near container corner (chosen coordinates  $x = 0,014$  m,  $y = -0,014$  m) is displayed by dash line. The dependence for line in half of container wall is displayed by solid line. Lorentz forces values are divided by maximum of Lorentz forces for Taylor number  $10^6$ . In Fig. 8 there is dependence of Lorentz forces on Taylor number. With increasing Taylor number Lorentz forces are larger. In Fig. 8 there is clearly to show how larger Lorentz forces near corner are.

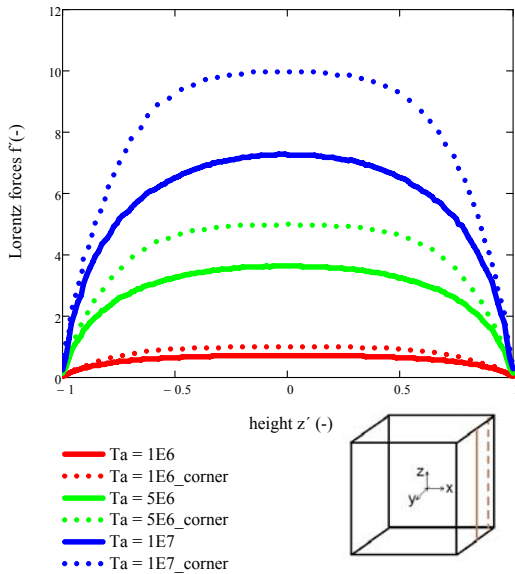


Fig. 8 Dependence of Lorentz forces on non-dimensional height of the container for different Taylor

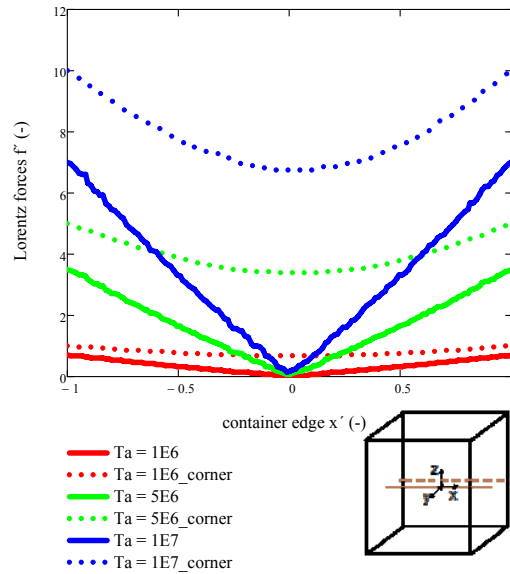


Fig. 9 Dependence of Lorentz forces on non-dimensional edge of the container for different Taylor

In the area of solid line Lorentz forces is increased from  $Ta = 1.10^6$  to  $Ta = 5.10^6$  approximately three times, from  $Ta = 5.10^6$  to  $Ta = 1.10^7$  approximately twice. In the area of dash line (line near container corner) Lorentz forces are much larger. With increasing Taylor number difference between Lorentz forces for solid line and dash line are larger. Increasing Taylor number is caused only by increasing magnetic induction (other magnitudes are the same). Magnetic induction directly affects Lorentz forces. That is the reason of increasing Lorentz forces with increasing Taylor number.

Dependence of time-averaged Lorentz forces (in azimuthal direction) on non-dimensional container edge is displayed in Fig. 9. Graphs by solid line are displayed for horizontal line passing through coordinate basic origin in half of container height. Graphs for dash line are displayed for horizontal line near container wall (chosen coordinates  $z = 0, y = -0.014$  m). Lorentz forces values are divided by maximum of Lorentz forces for Taylor number  $10^6$  as well. In the area of coordinate basic origin Lorentz forces are almost zeros (no mass, no momentum). Lorentz forces are much larger in the area of dash line. The ends of dot lines in graph of Fig. 9 are placed to area of higher Lorentz force, because both ends of the line are placed near corners. Graphs displayed by solid lines have linear dependence (from zero to maximum on both sides near walls). With increasing distance from vertical axis to container walls Lorentz forces are larger. With increasing Taylor number Lorentz forces are larger as well. Graphs displayed by dot lines do not have linear dependence.

Contours of velocities for Taylor number  $Ta = 1.10^6$  and  $Ta = 5.10^6$  are obtained similar. Only values of velocities are larger for  $Ta = 5.10^6$ . Change of Taylor number from  $Ta = 1.10^6$  to  $Ta = 5.10^6$  is caused by increasing magnetic induction from  $B_0 = 4.478.10^{-3}$  T to  $B_0 = 0.01001313$  T.

*B. Velocity for Different Taylor Number*

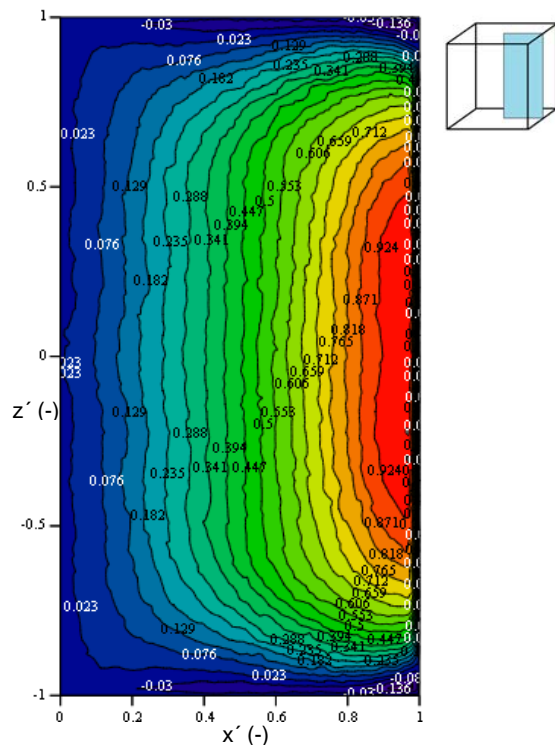


Fig. 10 Contours of time – averaged azimuthal velocities in central plane for  $Ta = 5.10^6$

In horizontal axis and vertical axis non-dimensional cuboid edge size  $x'(-)$  and  $z'(-)$  are used as well (Figs. 10–12). Because of symmetry only half of the container section is displayed. Contours of Lorentz forces for  $Ta = 5.10^6$  are very similar to  $Ta = 1.10^6$  (only larger values). That is the reason

of very similar contours velocities for  $Ta = 1.10^6$  and  $Ta = 5.10^6$  (only larger values).

Contours of velocities are similar for  $Ta = 1.10^6$  and  $Ta = 5.10^6$ . Differences are in values of velocities. Larger velocities are obtained for larger Taylor number.

V.CONCLUSIONS

In this work Lorentz forces in cuboid container were described. Contours of Lorentz forces were displayed in different plane of the container. Caused velocity fields were displayed for different Taylor number. Maxima and minima of Lorentz forces and caused velocity field were found. Dependence of Lorentz forces on height of the container and edge of the container for different Taylor was displayed as well.

REFERENCES

- [1] P. A. Davidson: "An Introduction to Magnetohydrodynamics", Cambridge, 2001.
- [2] P. Dold, K. W. Benz: "Rotating magnetic fields: fluid flow and crystal growth applications".
- [3] R. Möbner, G. Gerbeth: "Buoyant melt flows under the influence of steady and rotating magnetic fields", Journal of Crystal Growth, 1999.
- [4] K.-H. Spitzer, "Application of Rotating Magnetic Fields in Czochralski Crystal Growth", Progress in Crystal Growth and Characterization of Materials 38, pp 39-58, 1999.
- [5] L. M. Witkowski, J. S. Walker: "Flow driven by Marangoni convection and Rotating Magnetic Field in a Floating – Zone configuration", Magnetohydrodynamics, Vol. 37, 2001.
- [6] E. Yildiz, S. Dost: "A numerical simulation study for the effect of magnetic fields in liquid phase diffusion growth of SiGe single crystals", Journal of Crystal Growth 291, 2006.
- [7] Doležal I, Musil L.: "Modern industrial technologies based on processes in fluid metal controlled by electromagnetic field", 11/2003, Praha, 2003.
- [8] K. Fraňa, J. Stiller, A numerical study of flows driven by a rotating magnetic field in a square container, European Journal of Mechanics - B/Fluids, Issue 4, Vol. 27, 2008, p.p. 491-500.
- [9] K.Fraňa, V. Honzejk, K. Horáková: "A numerical simulation of the magnetically driven flows in a square container using the Delayed Detached Eddy Simulation", Sixth International Conference on Computational Fluid Dynamics, St. Petersburg, Russia.
- [10] K. Horáková, K. Fraňa: "Lorentz forces of rotating magnetic field", Mechanical Engineering Journal Strojárstvo, 2009, Slovak Republic
- [11] K. Horáková, K. Fraňa, "The effect of Lorentz forces parameters", Experimental fluid mechanics 2009, Liberec, Czech Republic.
- [12] J. Priede, "Theoretical study of a flow in an axisymmetric cavity of finite length driven by a rotating magnetic field", Ph.D. thesis, Institute of Physics, Latvian Academy of Science, Salaspils, 199.
- [13] K. Horáková, K. Fraňa, "Energetic spectra of unsteady flows", Journal of Applied Science in the Thermodynamics and Fluid Mechanics, No. 1/2011.

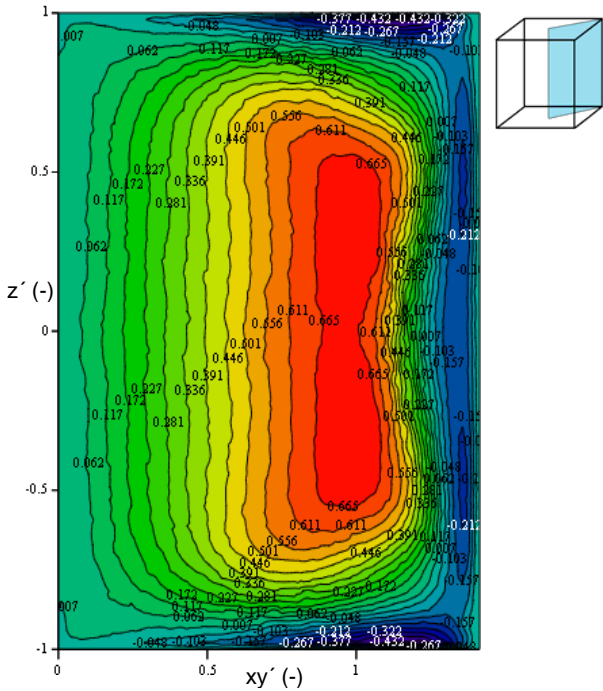


Fig. 11 Contours of time – averaged azimuthal velocities in cross plane for  $Ta = 5.10^6$

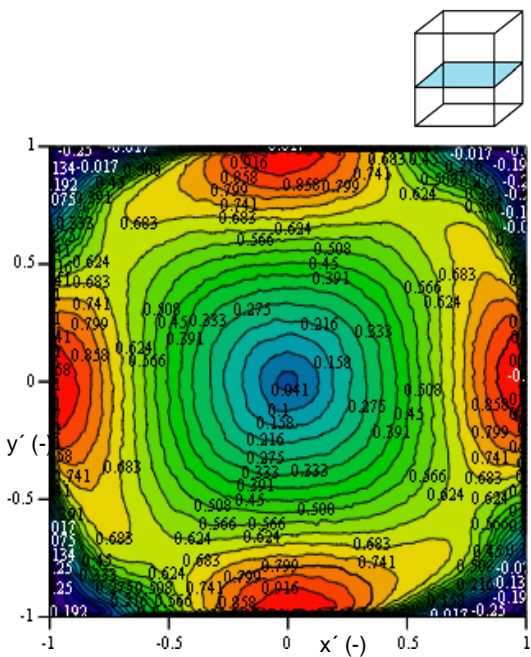


Fig. 12 Contours of time – averaged azimuthal velocities in horizontal plane for  $Ta = 5.10^6$